Journal of Manufacturing Processes 74 (2022) 52–62

Contents lists available at ScienceDirect

Journal of Manufacturing Processes

journal homepage: www.elsevier.com/locate/manpro

Applied computer vision for composite material manufacturing by optimizing the impregnation velocity: An experimental approach

Juan-Antonio Almazán-Lázaro *, Elías López-Alba, Francisco-Alberto Díaz-Garrido

Department of Mechanical and Mining Engineering, Campus Las Lagunillas, University of Jaen, 23071 Jaén, Spain

ARTICLE INFO

Keywords:
Computer vision
Optimization
Manufacturing
Control
Mechanics
Composite
Materials

ABSTRACT

The application of the cutting edge industrial solutions in composite manufacturing are optimizing the processes, quality control and resources usage. Computer vision is currently used in many quality control stages, although its potential advantages have not been applied in the process control. In this paper, computer vision is used to control the impregnation velocity in VARI (Vacuum Assisted Resin Infusion) process. As it is known, there is a relationship between the impregnation velocity and the final mechanical properties in LCM (Liquid Composite Manufacturing) processes. Constant and optimum flow front velocity mean optimum mechanical properties, although the nature of the process makes it difficult to keep these conditions. Then, a methodology has been proposed to identify and use the optimum velocity during the manufacturing process. Firstly, the flow front recognition algorithm was calibrated to be used in different reinforcement and fluid systems. Then, tensile and impact specimens have been manufactured and tested at different controlled and uncontrolled velocities. As a result, the tensile modulus has been increased up to 12.6%, as the tensile strength has increased up to 8.7%. Similarly, the maximum reaction force during the impact test has been increased up to 6.5%, as the damaged area has been reduced by 8.8%. For stitched laminates, force results increase up to 3.2%, as the damaged area has been reduced up to 31% when the optimum velocity is used. The experimental results have demonstrated the advantage of using mechanisms to control the impregnation process to achieve improved mechanical properties of composite materials.

1. Introduction

The increasingly use of resources in the industry is resulting in the encouragement of emerging innovations to control the production. The waste reduction, the quality refinement, the manufacturing flexibility and the reduction in the operation costs are the goals of the industry 4.0. To cover these challenges, technologies such as machine learning, IoT (Internet of Things) devices and data exchange are being intensely used nowadays. Computer vision is one of the most common way to collect data in many industrial processes, due to its flexibility and the large amount of collected data. In the industry, most of applied vision system are being used for inspection or quality control, but only limited literature is available about direct applications for manufacturing processes control, specifically in materials manufacturing.

In the composite manufacturing industry, Vacuum Assisted Resin Infusion (VARI) or RFI (Resin Film Infusion) process is one of the available methods to manufacture parts. It is framed into LCM (Liquid Composite Moulding) techniques which are based on the impregnation of the initially dry fibres using a mould and pressure. Specifically, VARI involves a semi-mould which is covered and sealed by an airtight bag which leads to a cost-effective process for large parts. The staking of dry fibres is placed over the mould geometry before the sealing and then the resin and vacuum ports are plugged into the bag. As the vacuum is applied, the resin flows from the resin pot to the vacuum line and the dry fibres are getting impregnated. The material quality and performance is directly related to the manufacturing process parameters. As it is known, the increase in the mechanical properties means a weight reduction as well as increase of energy efficiency and parts handling. Then, the process control is crucial to achieve optimum and repetitive properties in the materials. As highlighted by Ashir et al. [1], dry areas, unsaturated areas and voids, which are very common, reduce the mechanical properties as the weight increases consequently due to more material should be used. As it has been reported by Leclerc and Ruiz [2], there is a relationship between the impregnation velocity (i.e. flow front velocity: the rate at which the fibres are impregnated) and the final mechanical properties. This effect is highly relevant in dual-scale materials, in which

* Corresponding author.
E-mail address: jalmazan@ujaen.es (J.-A. Almazán-Lázaro).

https://doi.org/10.1016/j.jmapro.2021.11.063
Received 20 August 2021; Received in revised form 25 November 2021; Accepted 30 November 2021

fibres are arranged together in yarns. Then, two-scale flows are generated in these materials and capillary and viscous phenomena are in the background of the process. On the one hand, a microscopic flow is generated in the gaps among individual fibres where capillary effects manage the impregnation process. On the other hand, a macroscopic flow is generated through the macroscopic gaps among yarns. As a result, these two flows take place simultaneously. As reported by Leclerc and Ruiz [2], when one of these flows go faster than the another, voids are generated in the gaps of the slower flow. The viscous flow, which is managed by the applied pressure, could be modified as the process parameters are changed. Then, there is an optimal impregnation velocity in which both flows are equal and void are not generated or the amount is minimised: the optimum flow front velocity. This optimum value match with the value at which the maximum mechanical properties are reached as it was recently reported by Leclerc and Ruiz and [2] and Almazán et al. [3] for tensile loads. Hence, the ideal impregnation process is the one which keep the flow front velocity during the whole process.

Then, in VARI (Vacuum Assisted Resin Infusion) techniques, parameters such as pressure, viscosity, temperature, vacuum level modifies the flow behaviour. Also the fabric parameters such as permeability, thickness or compressibility will introduce different pressure losses which modify the flow. Furthermore, the geometry of the part and the inlet/outlet ports change the flow characteristics. For these reasons, a reliable method is required for VARI process to guarantee that the impregnation process is properly performed. The Darcy model for porous media [4] is used to describe the flow behaviour in the space and time. Then, some software is commercially available to foresee how the flow front is going to be developed, although most of the input parameters are difficult to measure experimentally as highlighted by Mesogitis et al. [5]. Also, the low production rates make the standardization difficult. In this context, the in-situ measurements of each process is one of the most potentially applicable and feasible methods to control the process.

In the literature, the work of Zambal et al. [6] applied a vision system to evaluate the quality in AFP (Automatic Fibre Placement) to detect gaps and overlaps automatically. Similarly, Juarez et al. [7] and Denkena et al. [8] used thermographic cameras to detect similar defects. Jeyaraj and Samuel Nadar [9] also showed an application for defects detection and classifications in fabrics. Hulagadri [10] also showed the application of computer vision in injection moulding. Another related research was performed by Lekanidis and Vosniakos [11]. They reported a successful computer vision system to manage the impregnated areas in VARI systems, aiming to avoid dry areas, especially for multiple inlet cases.

Although alternative methods to monitor the flow have been reported for many authors, they have not been used to control the process. Then, Carlone et al. [12] and Pouchias et al. [13] show a well-correlated and non-invasive method based on dielectric measurements. Optical fibres have also been used by Gupta and Sundaram [14] for in-plane and transverse detection of the fluid flow front during the LRI manufacturing process, although their handling and moulds are not cost-effective. In all cases, the industrial implementation requires from complex moulds that should be renewed for every new geometry. Similarly, Danisman et al. [15] measured the flow through voltage sensors, and Moghaddam et al. [16] used pressure embedded sensors in VARI. Also, embedded thermocouples have been also used for flow monitoring, especially in those cases which temperature of resin is different from the mould, as shown by Wang et al. [17]. Although embedded sensors could provide high accuracy, they work as stress concentrators in the materials and mechanical properties are drastically deteriorated as described by Moghaddam et al. [18]. Other techniques based on cameras were used by Govignon et al. [19] to monitor the thickness and derived parameters during the impregnation in RTM. Similarly, Ravey et al. [20] used an infrared thermographic camera to visualize the flow in non-transparent fibres although it was not controlled. Also, Sas et al. [21] used a camera-based system to optimize the process by using a porous media. Some of these sensors are based on lineal sensing, which allow to monitor only in the line where they are placed. Examples of these sensors are optical fibre or electrical sensors. On the other hand, some areal sensing methods are also available, including piezoelectric and dielectric sensors. In all cases, the accuracy is highly dependent on the number of sensors.

As a full field technique, the computer vision can be potentially applied in analyzing the flow features such kinematics parameters, shape and derived defects as racetracking or flow hesitations. This proposed technique reduces the mould cost due to it is based on an external device and only repositioning and optical-adjustment may be required. Additionally, this non-intrusive technique avoids any likely reduction in the mechanical performance of the composite. Other point-techniques such as embedded pressure sensors, optic fibres, capacitive or piezoresistive sensors are only valid to track the flow point by point [22]. Consequently, these techniques are not valid to control the flow since they are not able to provide data enough to keep the velocity controlled between the local measurements. In some specific cases, continuous embedded capacitive sensors could provide an almost continuous data about the flow front profile [22]. In all cases, these last techniques imply extensive cost in the tooling. The cost-effectiveness of visual observation using cameras was highlighted by Moghaddam et al. [16], who also remarked the high tooling cost of localized sensing in the moulds and agree with Konstantopoulos et al. [23].

As a disadvantage of the proposed system, it could be highlighted that the high porous media at the top of the laminate could generate some velocity gradients through the thickness. The delay between the fully impregnated area and the dry area has been described by authors such as Mehdikhani et al. [24], and in all cases, the layer velocity is the same, despite the delay. Even though, the optimum flow front velocity will be previously evaluated, before the final impregnation. Then, these effects are taken into account, whatever the stacking be.

The Darcy equation for porous media [4] can be used to model the flow behaviour during the impregnation process. The unidimensional model is shown in the Eq. (1), where u is the flow front velocity (i.e. impregnation velocity), K is the unidirectional permeability, $\Delta P/\Delta x$ is the applied pressure gradient, μ is the dynamic viscosity and $\varnothing$ is the media porosity. Since the pressure gradient is continuously changing as the flow position changes, the flow front velocity is also continuously changing.

$$u = \frac{\Delta P \cdot K}{\Delta x \cdot \mu \cdot \varnothing} \tag{1}$$

Unlike RTM, where flow rate could be controlled easily in the injection pump, in VARI process is not as easy. The ΔP is constant during the process and it is defined by the difference between the atmospheric pressure and the vacuum pressure (usually near zero). The distance travelled by the flow front, Δx, is always raising. As the rest of variables are constant properties of fabric and resin, the flow front velocity is following an inversely proportional relation to flow position, and it is not easy to impose this relation in the vacuum pump. Similarly, the velocity is changing with the time, and it is defined by (Eq. (2)). Because of this complexity, computer vision may be one of the most effective ways to control the impregnation velocity, keeping it in constant and optimum values during the whole process.

$$u = \sqrt{\frac{\Delta P \cdot K}{\Delta t \cdot \mu \cdot \varnothing}} \tag{2}$$

As a consequence, the instantaneous flow front position is not linear as it is given by Eq. (3), according to theoretical definitions as shown by Masoodi et al. [25] and numerically by Hattabi et al. [26]. Additionally, since the parameters of permeability, viscosity and porosity are likely to change at each area of the laminate, high complexity is found in the flow controlling.

$$x = \sqrt{\frac{2 \cdot \Delta P \cdot K}{\mu \cdot \varnothing} t} \tag{3}$$

In this work a methodology to control de flow front velocity during the impregnation processes is presented using a full field computer vision system. The highly complex process of controlling the flow is faced using an experimental approach in this methodology. Then, the application of the computer vision allows to minimize de defect generation and improved mechanical properties are achieved consequently.

2. Materials and methods

The proposed methodology is based on controlling the flow front velocity during the impregnation process. An adjustable valve is continuously managed by the computer vision system in a closed loop. After the image processing and flow recognition, the response of the image processing is applied over the valve to keep the flow front velocity at the optimum velocity.

2.1. The control system

To measure the flow front velocity and adjust the flow rate afterwards, an algorithm and a hardware have been specifically developed. A double approach has been considered to keep the flow front velocity in the previously set value. Firstly, the flow position was continuously evaluated and compared with the position where the flow should be found if it goes at the set velocity. Additionally, the velocity was also evaluated continuously and compared to the optimum value. Both measurements are read by the controller system, which provides the valve position as output. The global processing flowchart is shown in Fig. 1. Once the algorithm is started, the calibration parameters such as distortion corrections according to the lens type and laminate distance are included. Also, the goal value for the velocity is specified (usually it correspond to the known optimum velocity for the specific laminate). Once the lighting conditions have been stablished, a first picture is taken as a reference, and the vacuum is applied. As impregnation starts, the camera is continuously taking pictures of the laminate area. Then, the flow recognition algorithm is applied to locate the flow position in the image. Taking into account the previously set calibrations, the real position is assessed for the specific time, $\overline{x_{inst}}$. The line over the variable in this context means the average value across the flow front domain. By measuring the time between consecutive images, the flow front velocity is also evaluated, $\overline{u_{inst}}$. A 5-points mean filter is applied to avoid noisy values. After calculations, the actual values are compared with the optimum ones: flow position and velocity. Using this information, the PID system controls the valve position. If the flow front position and velocity is lower than the optimums, $x_{opt} \pm \Delta$ and $u_{opt} \pm \Delta$, the valve will be opened to increase the flow rate and vice-versa. The value Δ is previously set (usually 10%) as admissible variations in the range of values.

The specific flowcharts are shown in Fig. 2. According to the region of interest, the acquired image is firstly cropped to remove the pointless information around the laminate edges while boosting the calculation performance. The central area of each laminate was fixed as region-of-interest to measure the flow front velocity. Then, effect such as race-tracking was avoided to affect the measurements. To reduce the image distortions, the Scaramuzza [27] algorithm has been used. It was previously calibrated and its parameters were determined for this specific implementation. Additionally, every image was equalized because the original images do not display a suitable contrast. After that, the difference in the pixel intensities was enhanced and the flow font was easy-to-detecting. Once the process starts and the laminate is still unimpregnated, one image is initially taken and it is set as a reference during the whole process. For every single image taken during the process, this initial image was subtracted and the impregnated area is highlighted (Eq. (4)).

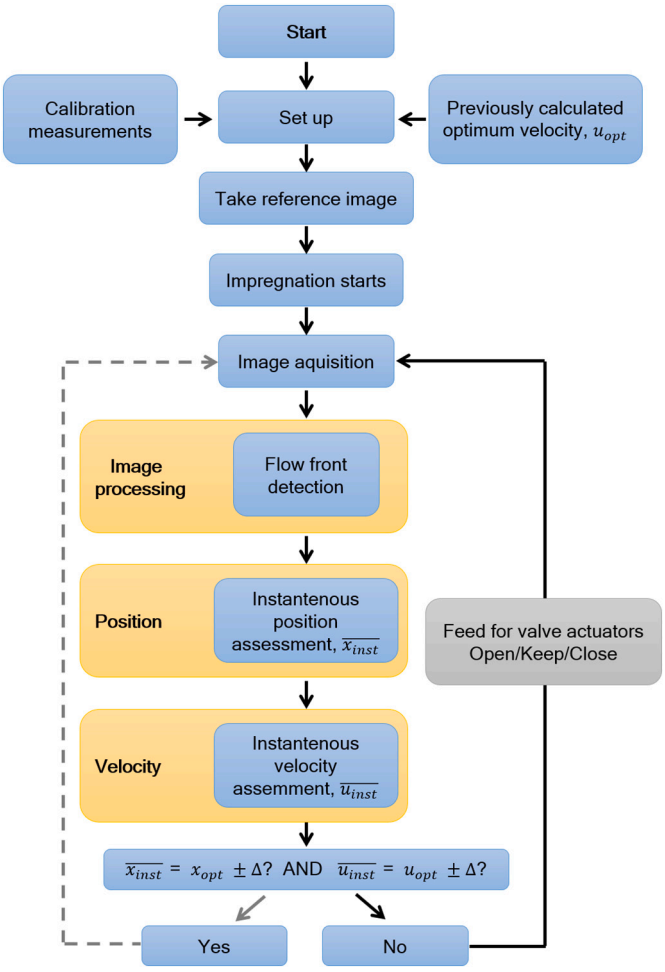

Fig. 1. Global processing flowchart.

$$D(x, y) = |I(x, y) - I_0(x, y)| \tag{4}$$

where $D(x,y)$ is the subtracted image, $I(x,y)$ is the acquired image, and $I_0(x,y)$ is the initially acquired image from the unimpregnated laminate, and (x, y) is the pixel position.

Then it is converted to grayscale and [5 × 5] mean filter is applied to reduce the noise. The unimpregnated areas will show intensities near-to-zero while the new-impregnated areas will show highest values. The flow front position could be easily detected as the edge in which the intensity values changes from near-to-zero to a positive value. The base-on-gradient Sobel method is used to segment the images and highlight the flow line. Since some noise has been reported at this time, the result is eroded and dilated. Then, the whole image is segmented and the small areas are removed to isolate the flow front line. Using this result, the average flow position of the actual image is evaluated. Once the flow has been located in the image, the previously calibration inputs are used to convert the image position into real length position at each time $\overline{x(t)}$. Finally, the position data is used to evaluate the instantaneous velocity $\overline{u(t)}$. It requires the time between two consecutive images, t and t_0 as well as the corresponding flow position $\overline{x(t)}$ and $\overline{x(t_0)}$. All of the algorithms were implemented in Matlab, and a GUI (Graphical User Interface) were developed to manage all parameters during the processing, the calibration and the data acquisition. Some adjustment capabilities were added to make the algorithm general-purpose, and adjustments for brightness, contrast and gamma levels were added.

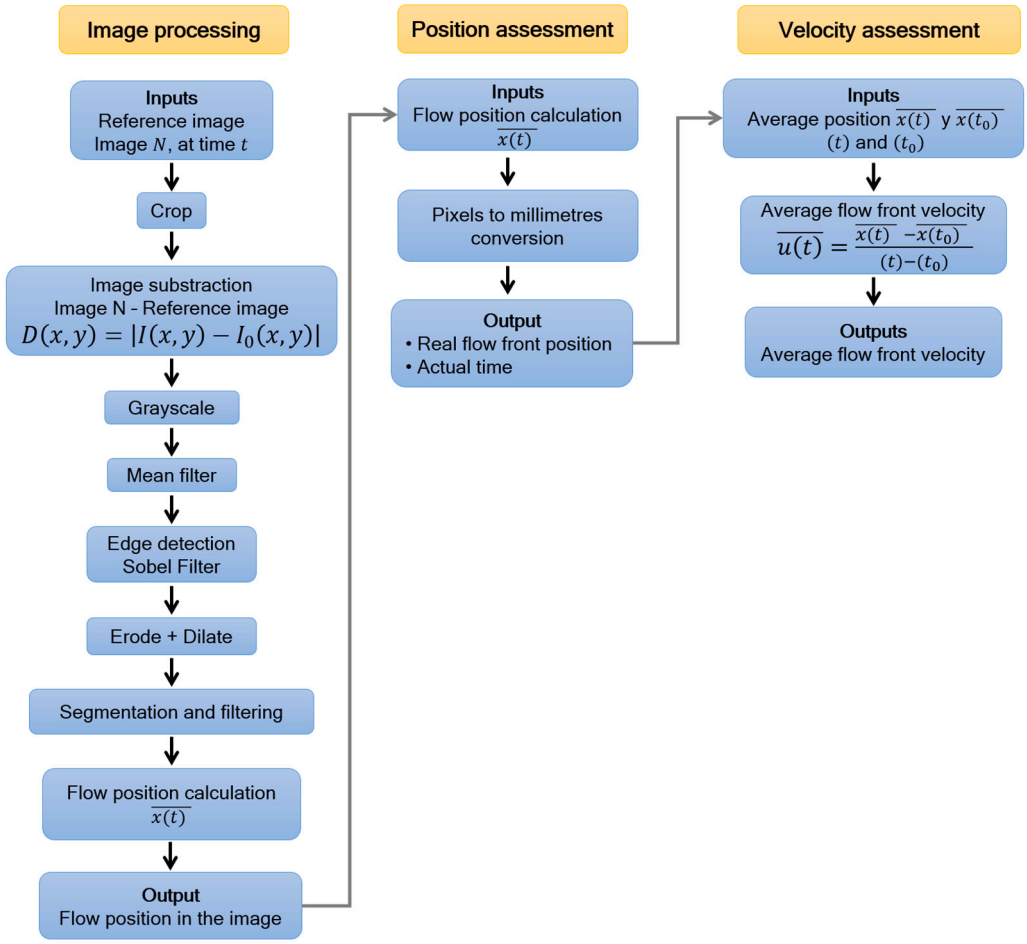

Fig. 2. Flowchart for image processing (left), flow position (center) and velocity (right).

2.2. Setup and equipment

The setup schematic is shown in Fig. 3. The mould with the dry fibres inside is connected to the vacuum pump and the resin pot as per conventional VARI process. Over the mould, a camera and a set of lights are properly positioned using supports. Additionally, a position-controlled valve is placed in the vacuum hose. The valve and the camera are connected with a computer. An algorithm is continuously reading the shots from the camera at the same time it assesses the real position and velocity of the flow front. Both values are compared with the previously set optimum values.

The setup, including the mould, was enclosed by an opaque wood-made box aiming to avoid any influence from the external lighting (Fig. 3). Since controlled lights were included inside, the illumination parameters can be kept constant during the process while the only change is associated to the flow front movement. It makes the flow detection easier. A specifically designed valve have been used in this methodology to control the flow by using the signals from the algorithms (Fig. 4). It allows to change the valve once the process is finished, avoiding to change the whole valve once the resin is cured. The servo-valve is managed by two parallel stepper servos which allow an accurate positioning. A rotational resistor has been used to read the actual position. A gear box has been used to reduce the output rotational velocity by 25 times as the torque is increased.

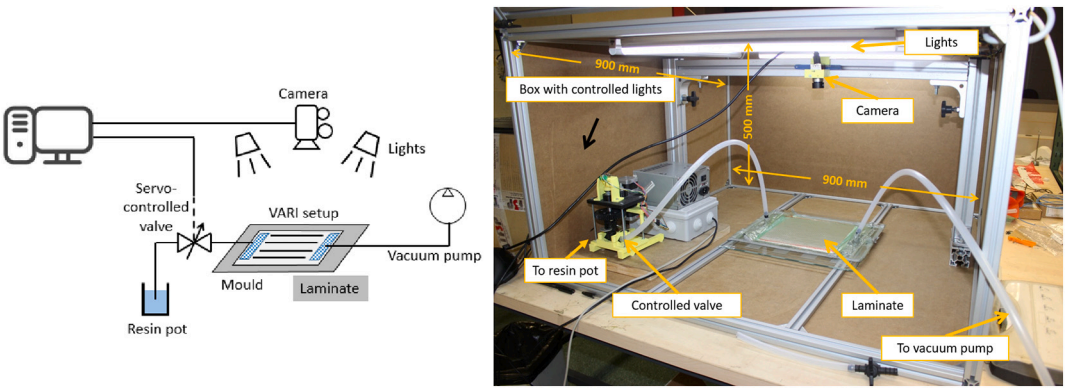

Fig. 3. Schematic view of the setup (left), and setup for the controlled impregnation in VARI (right).

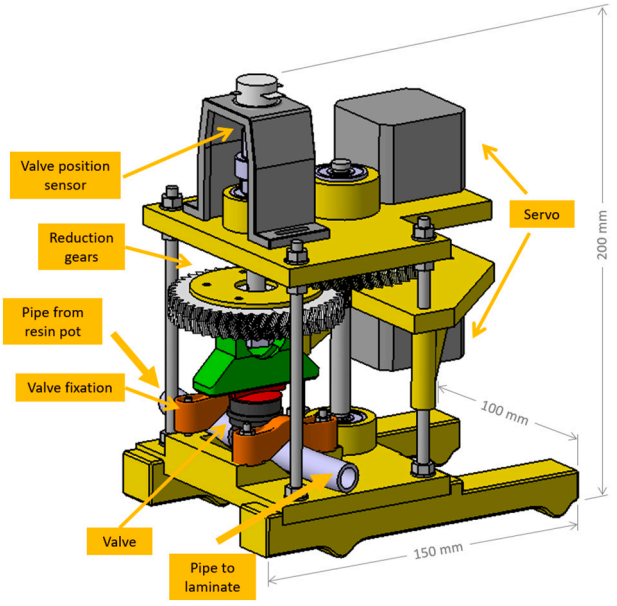

Fig. 4. Diagram of the developed hardware to control the flow.

To manufacture the laminates, a 2 mm thick steel plate has been used as mould base. E-glass fibre (600 g/m^2) was placed according to the defined stacking after applying was as a demoulding. A peel ply and a high porosity layer (1.19 mm and 135 g/m^2, from Dianet) were set over the fibre stacking. Plane channels (50 mm × 4 mm, Diadrain) were placed at the ports and polyethylene T-connections were used to plug Ø12 hoses. The nylon-based vacuum bag of 75 μm (BF-32 Wrightlon® from Airtech Inc.) was sealed using AT200Y tape (Airtech). A polyester-based resin (P4 TV-28, (Shaffhausen, Switzerland)) was catalyzed with M312 (Curox, Pullach, Germany) at 2% weight. To generate the vacuum level, a two-stage Edwards 80 vacuum pump was used and a resin pot (Airtech) was plugged to protect the pump.

In the computer vision system, a Mako 130B monochrome camera (Allied Vision, Stadtroda, Germany) was adopted to capture the flow front. The data was processed in Matlab and it was managed by the developed adjustable valve. The algorithm was executed with an Intel Core i5 7200 CPU 2.7 GHz processor and 4 Gb RAM with result in a frame-rate processing of 10 Hz. A wood-made box of 900 × 900 × 500 mm^3 were used to isolate the setup from any external lighting effect. A CNC sewing device (Pfaff 3574) was used to perform the stitching in the stitched laminates before the impregnation stage. Once the laminates were manufactured, the specimens were cut using a circular saw.

To evaluate the tensile material performance, a MTS 370.02 servo-hydraulic machine (MTS Systems Corporation, Eden Prairie, MN, USA) has been used. For impact tests, a drop tower of 15 m (Leibniz Institute for Composite Materials, Kaiserslautern, Germany) as well as 2 m drop tower (University of Jaén, Spain) were used. For these cases, a high speed camera (FASTCAM S4A 1024 × 1024 CMOS, Photron, Tokyo, Japan) was set, and the data was processed using VIC-2DTM to track the speckle and extract the impactor displacements.

2.3. Methodology

To evaluate the performance of the proposed method, preliminary tests were performed to adjust the setup and parameters. Firstly, a set of specimens were preliminary manufactured using different materials at uncontrolled velocities and the algorithms for detection were trained. Secondly, a range of tensile and impact specimens were manufactured in both unstitched and stitched configurations using controlled velocities. After testing, an optimum velocity was concluded according to the mechanical response of the materials.

In the first stage, the flow recognition system was tested. Unidirectional glass fibre $[0°]_2$ and a peel ply layer of 150 mm × 230 mm were impregnated with rapeseed oil. One unstitched laminate and one stitched laminate were used and the recognition algorithm were optimized in terms of image processing parameters. The flow position, velocity and time were acquired for processing and compare with Darcy predictions. The mean errors have been evaluated using the expressions in Eqs. (5) and (6), where x and u are describing the flow position and velocity and the subscripts are referred to the experimental measurements and the theoretical value from the Darcy model (Eqs. (2) and (3)), respectively. The value i is associated to the time at each experimental measurement.

$$\epsilon_{position,i} = \frac{x_{experimental,i} - x_{Darcy,i}}{x_{Darcy,i}} \tag{5}$$

$$\epsilon_{velocity,i} = \frac{u_{experimental,i} - u_{Darcy,i}}{u_{Darcy,i}} \tag{6}$$

Carbon fibre tape-based laminates of 100 mm × 200 mm were also impregnated using rapeseed oil. The goal is to analyze and guarantee the algorithm potentials covering a wide range of materials. Both unstitched and stitched laminate were tested. The data was also logged and compared with the Darcy predictions.

Then, the tensile specimens were manufactured. Unidirectional glass fibre of 200 mm × 300 mm was impregnated with polyester resin. In order to analyze the fibre orientation effect during the process and in the final mechanical properties, three different orientations were analysed: $[0°]_2$, $[45°]_2$ and $[90°]_2$. The position and velocity data were compared with the Darcy predictions. Then, the specimens were cut from the laminate and tested in a MTS universal testing machine, according to ASTM D3039 [28] standard. Since the flow front velocity is not constant during the impregnation, the specimens were cut according to the local flow front velocity depending on the position. Then, a wide range of velocities are available. The goal is to analyze the effect of the flow front velocity in the tensile properties. Once the optimum flow front velocity was assessed, the tests were performed using the optimum values as set-point in the controller for the three different fibres orientations.

Lastly, laminates for impact analysis were manufactured. In this case, the velocity controller was used to keep the flow front velocity constant during the whole impregnation. Low impact tests were also performed to validate the effect in out-of-plane loads. In order to have a reasonable inertia and out-of-plane properties, thicker stackings were used in these cases: $[0_2,90]_S$ and $[90_2,0]_S$. The last one was manufactured in both unstitched and stitched variations and then, the effect of the stitching were also tested. The stitching was performed automatically with a grid pattern with pitch of 3.3 mm and 10 mm between stitching lines. A range of velocities were set for both unstitched and stitched laminates, according to the Table 1. Taking into account that stitching allows to use higher velocities, slightly higher velocities have been set in these cases. In order to analyze the effect of the impact energy, two subsequent impacts were carried out, 13 J and 26 J. During the mechanical test, reimpact was prevented by holding the impactor after rebounding. As a result, the maximum reaction force in the impactor and the damaged area after the impacts were reported.

Table 1
Set values for the impact laminates manufacturing.

Ref.	Unstitched laminates	Stitched laminates
	Set-point velocity (mm/s)	Set-point velocity (mm/s)
V1	2.5	2.5
V2	4.0	5.0
V3	6.0	7.5
V4	11.0	13.5

3. Results and discussion

3.1. Preliminary flow characterization

Preliminary tests have been performed in order to validate the flow detection algorithm. Some results are shown in Fig. 5, where four flow positions have been represented. Rapeseed oil and glass fibre in $[90°]_2$ stack and peel ply at the top was used. The high contrast between the impregnated and unimpregnated areas are easily observed and recognized by the vision system. Especially at the beginning, some effects of racetracking are observed due to the asymmetry in the flow front. It was successfully detected by the algorithm. Image adjustments were set in the algorithm to maximize the contrast between both areas. These adjustments were kept for the next tests.

The acquired data have been represented in Fig. 6. Since normalized time has been used in both configurations and the length laminate are the same, position curves are close similar in both stitched and unstitched laminates. Nevertheless, the unstitched laminate took 408 s to be fully impregnated while only 56 s were required in the stitched case. Consequently, the velocity curves are dissimilar. This differences are related to the difference in permeability when stitching is added. The results have been compared to the predictions by the Darcy model. The permeability value, K, has been adjusted to fit the impregnation time from both experiments and Darcy model. The mean variation in the flow position was 10.5% in the unstitched laminate, and 3.2% was reported in the stitched laminate. Similarly, for the velocity, an average deviation of 22.1% was reported in the unstitched laminate while 22.8% was shown by the stitched laminate. These variations could be associated to the highest mean velocities due to low viscosity of rapeseed oil. The detection algorithm finds it difficult to measure the flow front position and velocity when the flow velocity is too high. Also, a very low viscosity fluid could induce some variations in the Darcy model due to different fluid behaviour. The observed noise in the velocity plot is higher than the observed in the position due to velocity is more sensitive to small time and position errors in the measurements.

Similarly, the results of the second analysis, when carbon fibre (CF) tape and rapeseed oil are used, are shown in Fig. 7. In these cases, the mean error was −14.2% for flow position and −0.6% for flow velocity in the unstitched laminate, and −2.4% for flow position and −2.3% for flow velocity in the stitched laminate. In these cases, the highly homogeneous fibre stacking reduces the mean error remarkably. Since the internal structure of the laminate is highly homogeneous, the flow characteristics are also more predictable as noise is minimised. In Figs. 6 and 7, the results of unstitched laminates show high deviation from the Darcy predictions. It is especially appreciable in the position graphs. Both cases have a very low permeability which implies a very limited effect of the applied pressure. Instead, the capillary effect is the predominant effect during the impregnation. Due to the monitorization of the flow front during the whole impregnation process, it can be concluded that at very low permeabilities, the Darcy model is not predicting the flow behaviour accurately.

Then, the potential of flow detection using a visible camera has been demonstrated. Nevertheless, other types of cameras could be used in a similar processing scheme, such as thermographic cameras for non-transparent moulds [20]. In any case, image techniques provide a more complete information about the flow behaviour, as soon as the camera frame rate is kept in a reasonable value. In this case, 10 Hz has reported a sufficient number of points to evaluate the position and velocity accurately.

3.2. Specimens manufacturing

In the third experiment, tensile tests have been carried out for unstitched specimens at different fibre orientations. Three different relative angles between fibres and flow were analysed: 0°, 45° and 90°. They were manufactured at uncontrolled velocity so as to have different flow velocities in the same locations of the laminates. According to Darcy's model, the flow front is decreasing as the position go further. Then, each impregnated laminate were split at different positions and the velocity were measured using the computer vision system. Due to the reduced width of the specimens, the assumption of constant velocity in the whole specimen can be assumed. A total of 15 specimens were cut for each fibre direction. Fig. 8 shows the flow front position and velocity measured for different fibre orientation measured from the impregnation direction: 0°, 45° and 90°. Similar curves were reported by Pouchias et al. [13] and Carlone and Palazzo [29] when they measured the flow in VARI process using dielectric sensors. The same figure also includes the predictions performed using the Darcy's model for both position and velocity. The mean error in flow position was 3.9% while the mean error for velocity was 15.5% for fibres at 0°. At 45°, the mean error in position was 3.8% and 14.6% in velocity. At 90°, 2.8% was obtained for position and 10.9% for velocity. It can be observed that the errors and deviations in position and velocity go down as the fibre orientation is changing from 0° to 90°. It can be explained when the absolute velocity value is taken into account. At high speeds, flow front changes very fast and the accuracy of the PID and vision system could be compromised. For lower flow fronts (e.g. fibres at 90°) the velocities are lower during the whole process and the system is able to measure the position and velocity accurately. The permeability at each orientation is defining the global velocity. From the Darcy model, $K = 1.92{\cdot}10^{-9}$ m^2 was estimated at 0°, $K = 1.13{\cdot}10^{-9}$ m^2 at 45°, and $K = 0.984{\cdot}10^{-9}$ m^2 at 90°. Then, according to experiments, the highest errors have been observed at the first stages of impregnation, where the velocities are much higher than in the rest of the process.

Subsequently, the specimens for impact test were impregnated. In this case, the flow controller was used to impregnate at constant flow

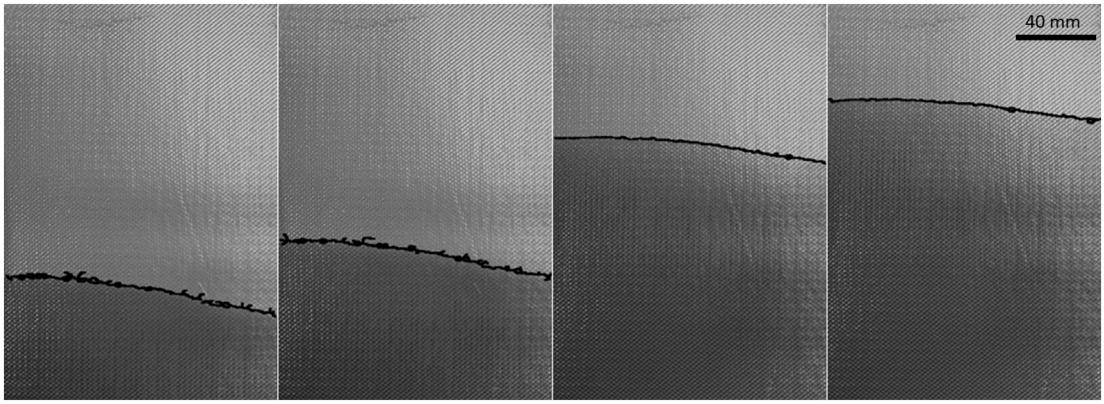

Fig. 5. Flow front recognition for $[0°]_2$ stacking at different flow positions when it flows upwards.

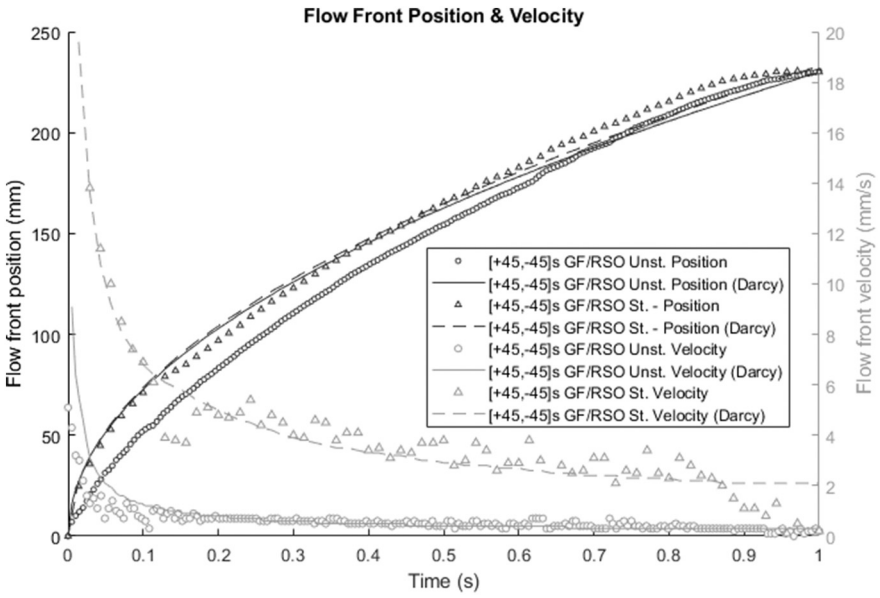

Fig. 6. Flow position and velocity in unstitched and stitched GF impregnated with rapeseed oil.

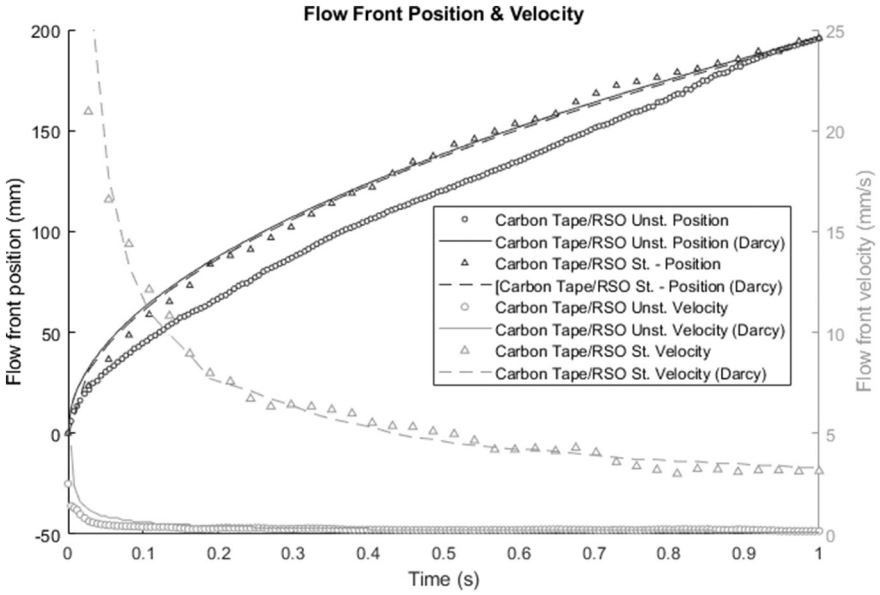

Fig. 7. Flow front position and velocity in unstitched and stitched CF Tape impregnated with rapeseed oil.

front velocity. A glass fibre $[0_2,90]_S$ and $[90_2,0]_S$ laminates was impregnated with polyester resin. Fig. 9 shows an example of the flow front position and velocity as a result of flow controller application. Also, the ideal position and velocity is shown as straight lines for 5 mm/s set point in the controller. The valve position is also shown at the bottom. As concluded from these figures, there is a direct relationship among the valve position, the instantaneous flow position and velocity. As the flow velocity and position increases over the goal lines, the valve is getting closer till complete blocking to reduce the flow. Once the velocity is crossing the goal line downwards, the controller starts to open the valve at different rates to compensate the flow velocity. Because the length of the laminate, the maximum achievable velocity is reached at the end. Although the controller read a velocity under the goal, it is not possible to increase the flow, even the valve is completely opened. This limitation is derived from the maximum impregnable length for this setup. As a consequence, the last part of the laminate is impregnated at velocities lower than the optimum value. By changing the laminate length, the porous media permeability, the resin viscosity or temperature, this limitation could be avoided and higher velocities could be achieved at the end of the process.

3.3. Tensile application

Tensile tests were performed afterwards to evaluate the stiffness and the strength of each configuration. The results are shown in the Fig. 10. Whatever orientation is analysed, there is a range of intermediate flow front velocities that lead to higher elastic modulus and tensile strength. These optimum values are within the range from 2 mm/s to 6 mm/s. Similar results were reported by authors such as Leclerc and Ruiz [2] in RTM, who also demonstrated that a minimum in void content means maximum mechanical properties. Similarly, in this case the results are getting worse as the impregnation velocity go further from the optimum range because of the void content is increasing. As expected, fibre orientation has a strong influence in both properties, especially for fibres

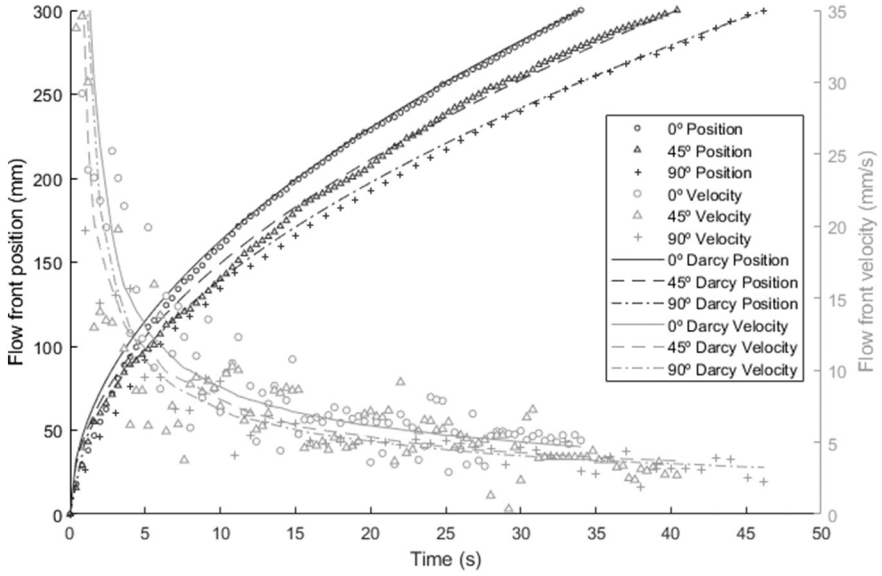

Fig. 8. Flow front position and velocity to validate the detection system when different fibre orientations are analysed through experiments and mathematical models in GFRP.

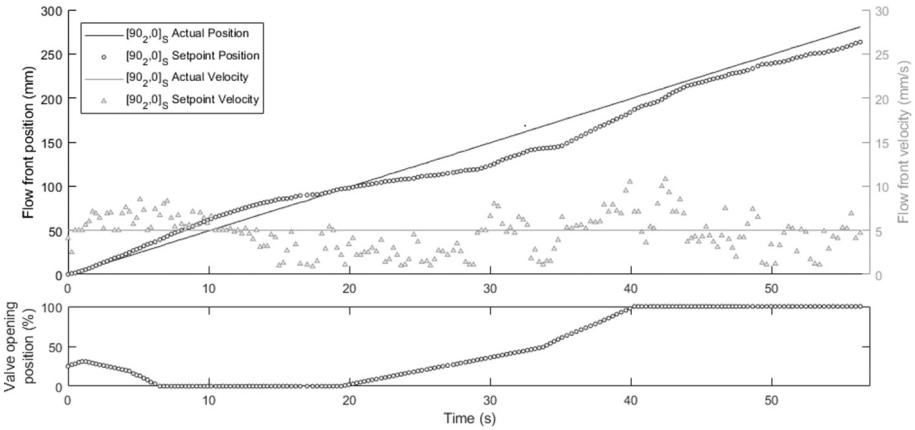

Fig. 9. Flow front position and velocity in $[90_2,0]_S$ stitched laminate when the flow controller is used (top); and valve position in the controller (bottom).

at 0° in which the fibre plays the most remarkable role. The average tensile strength was 191.4 ± 42.5 MPa at 0°, 69.8 ± 10.0 MPa at 45° and 45.7 ± 7.8 MPa at 90°. Similarly, the tensile modulus was 19.0 ± 1.4 MPa at 0°, 6.2 ± 0.9 MPa at 45° and 5.2 ± 1.1 MPa at 90°.

Once the optimum flow front velocity was assessed, the tests were performed using the optimum values as set-point in the controller for the three different fibres orientations. According to the results, the optimum flow front velocity was set in 4 mm/s. As a result of the tensile test, the tensile modulus was 20.1 ± 1.0 GPa, 6.9 ± 0.6 GPa and 5.6 ± 0.4 GPa for fibres at 0°, 45° and 90°, respectively. Similar trends were observed in the tensile strength: 225.4 ± 16.0 MPa, 73.2 ± 9.1 MPa and 47.2 ± 4.5 MPa for fibres at 0°, 45° and 90°, respectively. It means an increase in modulus of 12.6% on average in the tensile modulus and 8.7% on average in tensile strength. Although fibre orientation is modifying the optimum velocity results, there is not a clear relationship with the analysed values. Additionally, the repeatability of the results was increased, as the standard deviation were reduced by 44.9% for tensile modulus and 38.2% for tensile strength.

3.4. Impact application

For impact test, the four impregnation velocities which were set as set-point in the controller reports the real velocities shown in Table 2 for unstitched and stitched laminates. Small deviations were observed once the velocity data were analysed and compared with the set-points. These variations are associated to the PID inertia, the camera resolution, the processing rate and local variations in permeability which induce unpredictable velocity variations.

As a result of the impact tests, the maximum reaction force during the impacts were reported at each flow velocity. Fig. 11 shows the maximum reaction force at different flow front velocities when the specimens are impacted at 13 J and reimpacted at 26 J. The optimums values were found within the range from 3.5 mm/s to 6.5 mm/s. It could be explained if the void content is taken into account, as reported by Leclerc and Ruiz [2]. At 13 J, only a subtle increase in the reaction force is observed for intermediate velocity values. The maximum is located at 6 mm/s, where 3999.1 ± 15.6 N were measured, while the average value is 3949 ± 23.6 N. Nevertheless, a noticeable increase is reported in the case of the reimpacted specimens at 26 J. Maximum reaction forces were reached at the intermediate impregnation velocity of 6.0 mm/s (6512.0 ± 150.8 N) while the average value was 6147 ± 409 N. They mean an improvement of 1% at low energies and 6% at high energy impacts.

The damaged area were also reported, as shown in Fig. 11. In these cases, minimum values have been reported at 6.0 mm/s for high energy

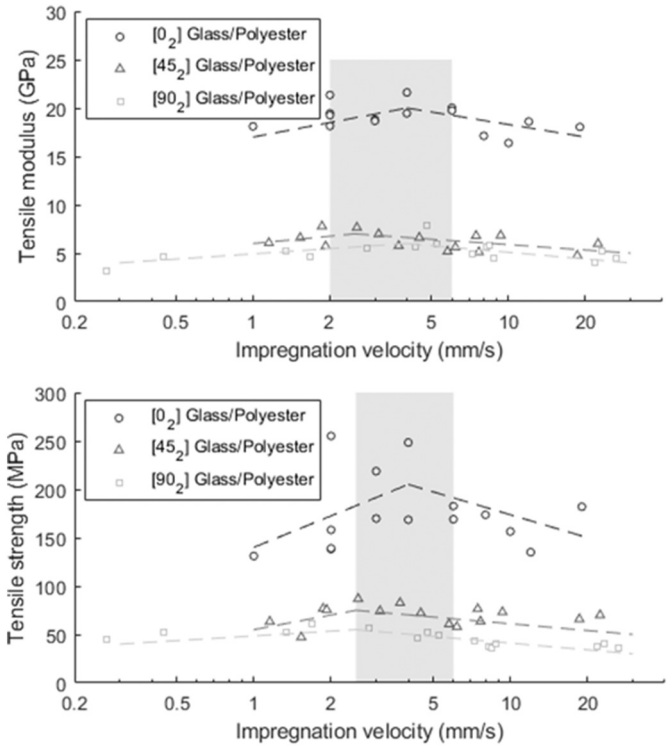

Fig. 10. Tensile modulus (left) and strength (right) in tensile test for the manufactured glass fibre/polyester specimens.

Table 2
Set values for the impact laminates manufacturing.

Ref.	Unstitched laminates		Stitched laminates	
	Set-point velocity (mm/s)	Actual velocity (mm/s)	Set-point velocity (mm/s)	Actual velocity (mm/s)
V1	2.5	2.5 ± 0.7	2.5	2.5 ± 0.7
V2	4.0	4.1 ± 0.5	5.0	5.2 ± 0.7
V3	6.0	5.9 ± 1.8	7.5	7.3 ± 1.6
V4	11.0	11.3 ± 0.5	13.5	13.7 ± 0.7

impacts, within the range of maximum reaction force. Damaged area is reduced from 6476 ± 1278 mm^2 on average to 5905 ± 776 mm^2 at 6 mm/s which mean a reduction of 8.8%. Again, only a subtle minimum is observed for 13 J impacts, from 2359 ± 509 mm^2 on average to 2206 ± 799 mm^2 that means 6.5% of reduction. From the low energy impacts, it can be concluded that the effect of the macrovoids is more reduced than the microvoids since a remarkable increase in damaged area is observed at high impregnation velocities up on the low velocities.

3.5. Application in stitched materials

Thirdly, impact tests were performed using stitched laminates. Similar trends were observed for intermediate values although the relative increase is less remarkable than the ones in unstitched configurations. At intermediate impregnation velocities of 4.5 mm/s and 8.0 mm/s, maximum values have been reported in both energy levels. On average, the maximum peak force was increased 3% on average, whatever impact energy was used. Regarding the stitching application, the peak force in stitched configuration is higher than the unstitched laminates using both energies. The relative improvement in these cases is lower than the unstitched configuration. It could be explained when the effect of the defects is taken into account. In stitched configuration, the relative effect of voids is partially hidden by the improvement of stitching. As shown, the dispersion of the data is higher in the case of high energy impacts. Due to the 26 J impacts is the second impact over the same specimens, some random effects appear such as impact point inaccuracies or position variations. Additionally, the variations during the stitching process or specimen preparation such as cutting or dimensional tolerances induces another variation source.

The damaged area was also reported for these cases (Fig. 12). The minimum damage area has been also reported at intermediate velocities at both impact energies. At 5 mm/s, 3324 ± 992 mm^2 were measured while the average value of all velocities is 3686 ± 880 mm^2. A similar improvement was observed at low energies, where 7.5 mm/s reported 1322 ± 329 mm^2 while the average value was 1928 ± 248 mm^2. It means a reduction of 9.8% and 31.4% for 26 J and 13 J impacts, respectively. The dispersion of the results is also higher in the case of 26 J impacts due to the random factors described above. When the stitched configurations are compared with the stitched configurations, a remarkable difference is observed as expected. At high impact energy, it is highlighted the positive effect of adding stitching, when the damaged area is reduced from 4858 ± 628 mm^2 to a mean value of 3324 ± 829 mm^2 that means a 31.6% or reduction from the unstitched configurations. At low energies, the effect of stitching is not statistically different. Indeed, no effect has been reported in the damaged area (Fig. 12), where the stitched results fits the unstitched results. It can be explained as the mechanisms under damage are taken into account. At low energies, the delaminations are limited to a small area where the interlaminar cracks can be propagated. In the unstitched configuration, the crack is managed by the fracture toughness of the laminate. In the stitched laminates, the stitching is limiting the crack propagation beyond the stitching characteristic length. In these cases, stitching is joining adjacent plies and limiting the crack propagation. At low energies, the delaminated area is not high enough to be extended beyond the seams, so the material toughness is managed by the interlaminar strength of the material. Since the local interlaminar strength is the same in both cases, no differences are observed between both configurations. It can be concluded that stitching has a positive effect in impact loads, especially at high energies, since it increases the stiffness and the damage tolerance. Additionally, the potential reduction of the damage area has been highlighted, especially at low impact energies. It could be associated to the local effects of micro and macrovoids. Low energy impacts generate a local damage that is managed by the local properties. High energies implies high deflections in the specimens and the effect of the defects are partially hidden by the high performance of the whole material. Then, stitching is not avoiding the crack generation, but it is able to limit its development.

To sum up the finding in this work, computerized vision can aid the composites manufacturing, maximizing the mechanical response as well as resources and sustainability are optimized. It has been highlighted the remarkable effect of the impregnation velocity on the mechanical properties. Although the reduction in void content is behind the basis of properties increasing, as other author reported in the past [2], the optimum impregnation flow front velocity can be assessed only by mechanical testing. Optimized impregnation velocities have improved the mechanical behaviour in both unstitched and stitched laminates for in-plane and out-of-plane loads. Stitching itself has boosted the mechanical behaviour for out-of-plane loads. A so-called “process windows” have been reported at velocities ranged from 2.5 to 7.5 mm/s where the maximum mechanical properties and minimum damaged were found. By using these velocities in the composite manufacturing industry, the mechanical properties will be improved and the required amount of material will be reduced consequently. By this methodology, the repetitiveness and the homogeneity of the results will be increased as the impregnation velocity is not depending on the flow position. Further analyses using multi-gate injection, weld lines, or complex geometries will boost its industrial application.

4. Conclusions

In this work, computer vision has been applied to control the

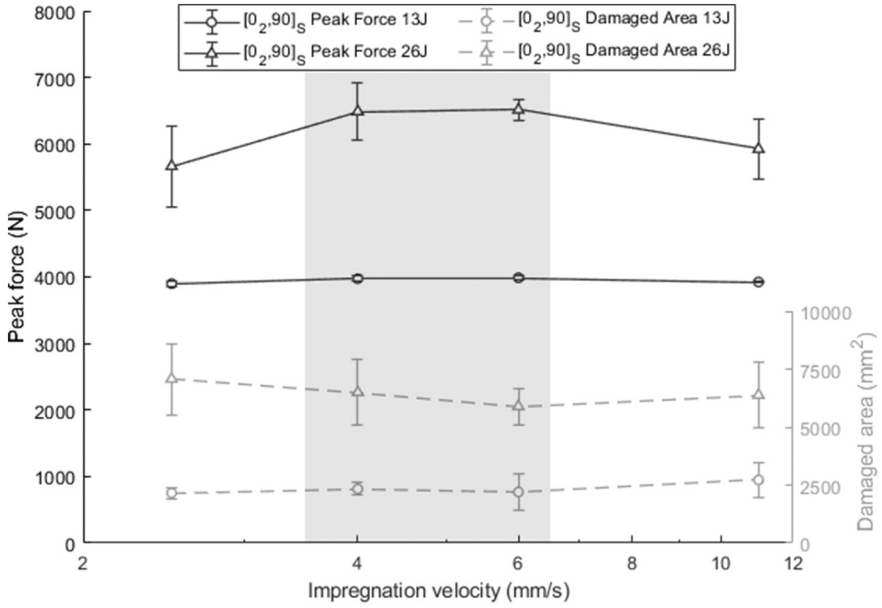

Fig. 11. Maximum reaction force at different flow front velocities when the specimens are impact at 13 J and reimpacted 26 J, and damaged area at different impregnation rates after 13 J and 26 J impacts.

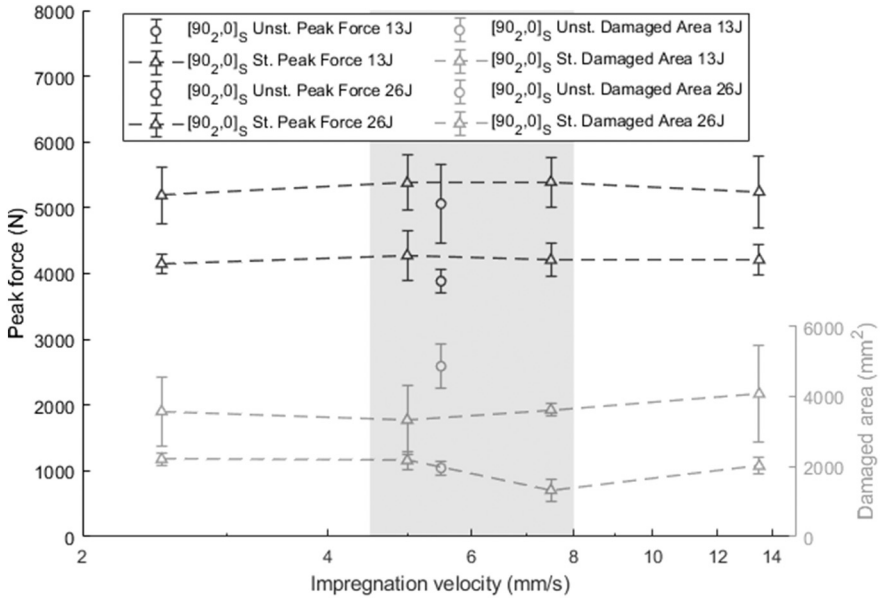

Fig. 12. Maximum reaction force at different velocities in stitched laminates for 13 J and 26 J impacts; and damaged area at different impregnation rates for impacts at 13 J and 26 J.

impregnation velocity in VARI processes. Since the mechanical performance is depending on the flow front velocity, it has been accurately measured and controlled at optimum values through computer vision. As a result, improved properties have been found for different load types and materials. The main conclusions of this work can be summarized as follows:

- Optimized tensile and impact properties have been found at intermediate impregnation velocities. A range of optimum velocities have been found in the so-called "process windows".
- The potential of flow detection using a visible camera has been demonstrated, and similarly, other types of cameras could be used for non-transparent moulds. In VARI processes, since the bag is usually transparent, the presented visible camera system is a highly cost-effective technique. Other techniques for non-transparent moulds imply extensive tooling cost or a punctual measurement approaches which have only limited accuracy.
- The methodology has been successfully applied over different stackings, sizes and commercial materials. Then, the approach could be extended to other configurations and its potential industrial applicability can be performed.
- On average, the tensile mechanical properties have been increased by 12.6% in module and 8.8% in strength, depending on the fibre orientation.
- The impact peak force in the unstitched laminated has been also increased up to 6% depending on the impact energy. Similarly, the damaged area after drop-impact have been also reduced up to 9%, depending on the impact energy.

- In stitched materials, the effect of optimizing the velocity is closely similar. The impact forces have been increased by 3% on average, whatever impact energy is used. The damaged area is also optimizable, and up to 31.4% of reduction can be achieved by velocity optimization.

By this novel approach using computer vision, the performance of composite materials manufactured by VARI can be improved. Therefore, as the control in the process is increased, lighter materials and more homogeneous results will be achieved.

Declaration of competing interest

The authors declare that they have no known competing financial interests or personal relationships that could have appeared to influence the work reported in this paper.

Acknowledgments

This research was supported by Airbus Defence and Space S.A.U. under Apolo project "*Alas de turbopropulsor mediante optimización logística y desarrollo online*" in the FEDER Interconecta Program.

References

[1] Ashir M, Nocke A, Bulavinov A, Pinchuk R, Cherif C. Influence of defined amount of voids on the mechanical properties of carbon fiber-reinforced plastics. Polym Compos 2019;40:E1049–56. https://doi.org/10.1002/pc.24820.
[2] Leclerc JS, Ruiz E. Porosity reduction using optimized flow velocity in resin transfer molding. Compos Part A Appl Sci Manuf 2008;39:1859–68. https://doi.org/10.1016/j.compositesa.2008.09.008.
[3] Almazán-Lázaro J-A, López-Alba E, Díaz-Garrido F-A. Improving composite tensile properties during resin infusion based on a computer vision flow-control approach. Materials (Basel) 2018;11:2469. https://doi.org/10.3390/ma11122469.
[4] Darcy H. Les fontaines publiques de la ville de Dijon: exposition et application647. Dalmont; 1856. https://doi.org/10.1080/00150199208223391.
[5] Mesogitis TS, Skordos AA, Long AC. Uncertainty in the manufacturing of fibrous thermosetting composites: a review. Compos Part A Appl Sci Manuf 2014;57:67–75. https://doi.org/10.1016/j.compositesa.2013.11.004.
[6] Zambal S, Heindl C, Eitzinger C, Scharinger J. End-to-end defect detection in automated fiber placement based on artificially generated data 2019;vol. 11172. https://doi.org/10.1117/12.2521739.
[7] Juarez PD, Cramer KE, Seebo JP. Advances in in situ inspection of automated fiber placement systems. In: Proc. SPIE. vol. 9861; 2016. https://doi.org/10.1117/12.2223028.
[8] Denkena B, Schmidt C, Völtzer K, Hocke T. Thermographic online monitoring system for automated fiber placement processes. Compos Part B Eng 2016;97:239–43. https://doi.org/10.1016/j.compositesb.2016.04.076.
[9] Jeyaraj PR, Samuel Nadar ER. Computer vision for automatic detection and classification of fabric defect employing deep learning algorithm. Int J Cloth Sci Technol 2019;31:510–21. https://doi.org/10.1108/IJCST-11-2018-0135.
[10] Hulagadri AV. Quality Classification of Defective Parts from Injection Moulding. 2020.
[11] Lekanidis S, Vosniakos G-C. Machine vision support of VARI process automation in composite part manufacturing. Int J Mechatron Manuf Syst 2020;13:169–83. https://doi.org/10.1504/IJMMS.2020.109799.
[12] Carlone P, Rubino F, Paradiso V, Tucci F. Multi-scale modeling and online monitoring of sesin flow through dual-scale textles in liquid composite molding processes. Int J Adv Manuf Technol 2018;96:2215–30.
[13] Pouchias A, Cunningham PR, Stein J, Kazilas M. Development of a flexible dielectric sensor for flow monitoring of the liquid resin infusion process. Sensors 2019;19:5292.
[14] Gupta N, Sundaram R. Fiber optic sensors for monitoring flow in vacuum enhanced resin infusion technology (VERITy) process. Compos Part A Appl Sci Manuf 2009;40:1065–70.
[15] Danisman M, Tuncol G, Kaynar A, Sozer EM. Monitoring of resin flow in the resin transfer molding (RTM) process using point-voltage sensors. Compos Sci Technol 2007;67:367–79.
[16] Moghaddam MK, Salas M, Ersöz I, Michels I, Lang W. Study of resin flow in carbon fiber reinforced polymer composites by means of pressure sensors. J Compos Mater 2017:1–10.
[17] Wang P, Demirel ÖM, Drapier S, Vautrin A. In-plane and transverse detection of the fluid flow front during the LRI manufacturing process. In: 9th Int. Conf. Flow Porc. Compos., Montreal, Canada; 2008.
[18] Moghaddam MK, Boll D, Lang W. Emedding rigid and flexible inlays in carbon fiber reinforced plastics. IEEE/ASME Int Conf Adv Intell Mechantron 2014:1387–92.
[19] Govignon Q, Bickerton S, Morris J, Kelly PA. Full field monitoring of the resin flow and laminate properties during the resin infusion process. Compos Part A Appl Sci Manuf 2008;39:1412–26. https://doi.org/10.1016/j.compositesa.2008.05.005.
[20] Ravey C, Ruiz E, Trochu F. Determination of the optimal impregnation velocity in resin transfer molding by capillary rise experiments and infrared thermography. Compos Sci Technol 2014;99:96–102. https://doi.org/10.1016/j.compscitech.2014.05.019.
[21] Sas HS, Simácek P, Advani SG. A methodology to reduce variability during vacuum infusion with optimized design of distribution media. Compos Part A Appl Sci Manuf 2015;78:223–33. https://doi.org/10.1016/j.compositesa.2015.08.011.
[22] Moghaddam MK, Breede A, Brauner C, Lang W. Embedding piezoresistive pressure sensors to obtain online pressure profiles inside fiber composite laminates. Sensors 2015;15. https://doi.org/10.3390/s150407499.
[23] Konstantopoulos S, Fauster E, Schledjewski R. Monitoring the production of FRP composites: a review of in-line sensing methods. Express Polym Lett 2014;8.
[24] Mehdikhani M, Gorbatikh L, Verpoest I, Lomov SV. Voids in fiber-reinforced polymer composites: a review on their formation, characteristics, and effects on mechanical performance. J Compos Mater 2018;53:1579–669. https://doi.org/10.1177/0021998318772152.
[25] Masoodi R, Pillai K, Grahl N, Tan H. Numerical simulation of LCM mold-filling during the manufacture of natural fiber composites. J Reinf Plast Compos 2012;31:363–78. https://doi.org/10.1177/0731684412438629.
[26] Hattabi M, Bensalah M, Echaabi J. Numerical and experimental analysis of the resin transfer molding process. Korea-Australia Rheol J 2008;20.
[27] Scaramuzza D, Martinelli A, Siegwart R. A toolbox for easy calibrating omnidirectional cameras. In: IEEE Int. Conf. Intell. Robot. Syst., Beijing, China; 2006. p. 7–15.
[28] ASTM International. ASTM D3039 - standard test method for tensile properties of polymer. Matrix Compos Mater 1995. https://doi.org/10.1520/D3039_D3039M-08.
[29] Carlone P, Palazzo GS. Unsaturated and saturated flow front tracking in liquid composite molding processes using dielectric sensors. Appl Compos Mater 2015;22:543–57. https://doi.org/10.1007/s10443-014-9422-3.